Polymer 247 (2022) 124789

Contents lists available at ScienceDirect

Polymer

journal homepage: www.elsevier.com/locate/polymer

Gas separation membranes obtained by partial pyrolysis of polyimides exhibiting polyethylene oxide moieties

Laura Matesanz-Niño [a,b], Carla Aguilar-Lugo [c], Pedro Prádanos [a], Antonio Hernandez [a], Camino Bartolomé [d], José G. de la Campa [e], Laura Palacio [a], Alfonso González-Ortega [b,*], Michele Galizia [f,**], Cristina Álvarez [a,e,***], Ángel E. Lozano [a,d,e]

[a] SMAP, UA-UVA_CSIC, Research Unit Associated to CSIC, Faculty of Science, University of Valladolid, Paseo Belén 11, E-47011, Valladolid, Spain
[b] Department of Organic Chemistry, Faculty of Science, University of Valladolid, Paseo Belén 7, E-47011, Valladolid, Spain
[c] Materials Research Institute, National Autonomous University of Mexico, University City, Mexico City, Mexico
[d] UI CINQUIMA, University of Valladolid, Paseo Belén 5, E-47011, Valladolid, Spain
[e] Institute of Polymer Science and Technology, ICTP-CSIC, Juan de la Cierva 3, E-28006, Madrid, Spain
[f] School of Chemical, Biological and Materials Engineering, University of Oklahoma, 100E. Boyd Street, Norman, OK, 73019, USA

ARTICLE INFO

Keywords:
Polyimides
Thermal cross-linking
Gas separation

ABSTRACT

Aromatic copolyimides (PIx) and aromatic-aliphatic copolyimides (PIxEOy) were synthesized by reacting 4,4′-(hexafluoroisopropylidene) diphthalic anhydride (6FDA) with mixtures obtained from 2,2′-bis(4-aminophenyl) hexafluoropropane (6FpDA), 5-diaminobenzoic acid (DABA) and Jeffamine ED-2003 (PEO).

The selective thermal removal of PEO from PIxEOy yielded membranes with high thermal stability and good mechanical properties. The presence of carboxylic groups minimized the shrinkage during the cross-linking process. The membranes containing 10 mol% DABA exhibited good O_2/N_2 and CO_2/CH_4 separation performance, and resistance to CO_2 plasticization.

PIx/PIxEOy blends containing less than 10 wt% PEO were prepared. The CO_2/CH_4 selectivity/permeability balance of cross-linked membranes largely exceeded that of PIx.

The results highlight a possible strategy for using analogous cross-linkable polymers exhibiting ethylene oxide moieties as mere additive to prepare high free volume polyimide's membranes, exhibiting enhanced separation properties and high resistance to plasticization.

1. Introduction

Separation and purification techniques may account for 70% of the costs in the chemical, petrochemical and pharmaceutical industry, therefore energy efficient, large scale separation processes are urgently needed to mitigate environmental pollution and improve social welfare [1–4]. Membrane gas separation offers interesting potential advantages over conventional separations (e.g., absorption, distillation, adsorption), including energy efficiency, small footprint, compact design and possibility to be integrated with other technologies, giving rise to process intensification [5–10]. The search for membrane materials exhibiting enhanced gas separation properties is being increasingly explored to improve existing applications (e.g., air separation, hydrogen recovery and CO_2/CH_4 and CO_2/N_2 separations), and develop new ones (e.g., olefin/paraffin separations and CO_2, H_2S removal from natural gas, separation at high temperature) [4,11–14].

The key factors determining the membrane performance for industrial gas separation applications are high selectivity (that is, the membrane's ability to discriminate a specific component in a mixture) and permeability (that is, the membrane productivity), adequate chemical, thermal and mechanical resistance under operating conditions, long working lifetime, cost-effective and defect free production. Glassy

* Corresponding author.
** Corresponding author.
*** Corresponding author. Institute of Polymer Science and Technology, ICTP-CSIC, Juan de la Cierva 3, E-28006, Madrid, Spain.
E-mail addresses: laura.matesanz@alumnos.uva.es (L. Matesanz-Niño), carla.aguilar.lugo@gmail.com (C. Aguilar-Lugo), pradanos@termo.uva.es (P. Prádanos), tonhg@hotmail.es (A. Hernandez), camino.bartolome@uva.es (C. Bartolomé), jcampa@ictp.csic.es (J.G. de la Campa), laura.palacio@uva.es (L. Palacio), alfonso.gonzalez.ortega@uva.es (A. González-Ortega), mgalizia@ou.edu (M. Galizia), cristina.alvarez@ictp.csic.es (C. Álvarez), lozano@ictp.csic.es (Á.E. Lozano).

https://doi.org/10.1016/j.polymer.2022.124789
Received 21 January 2022; Received in revised form 21 March 2022; Accepted 23 March 2022
Available online 25 March 2022

polymer membranes are mostly used in gas separations due to their desirable combination of size-sieving ability and mechanical properties. However, polymer membranes exhibit a well-known permeability/selectivity trade off, based on which highly permeable membranes are often poorly selective and vice versa. This behavior was evidenced by Robeson in 1991 [15], updated in 2008 [16], and revised recently [17–19], showing the progress in the area of membrane materials science [12,20]. Today, highly permeable membranes capable of surpassing the 2008 upper bound have been developed, such as aromatic polyimides [21], polymers of intrinsic microporosity (PIMs) [22,23], perfluoropolymers [24,25] and thermally rearranged (TR) polymers [26]. However, the issues of easy processability, mechanical stability and long-term stability are not yet solved.

Glassy high free volume polymers suffer from physical aging and plasticization, which limits their application in gas and liquid separations [27–30]. At temperature below glass transition temperature, short-range cooperative motions of polymer chains allow the system to slowly relax the excess free volume, to approach the final equilibrium state. Physical aging results in the polymer densification and, therefore, in a reduction of its internal free volume, which causes a decrease in gas permeability [31,32]. Plasticization is the consequence of polymer swelling upon sorption of highly condensable and soluble species, which translates to higher permeability and lower selectivity [28,33], and, analogous to physical aging, is related to chain mobility. Several approaches have been exploited to improve the resistance to plasticization and physical aging of high-free volume polymers [34] including, among others, polymer blending [35–37], chemical and thermal cross-linking [38–40] and addition of nanoparticles [29,41].

Cross-linking is one of the most cost effective and easy to apply strategy for reducing molecular mobility by increasing interchain rigidity and, thus, for mitigating physical aging and plasticization effects. However, cross-linked membranes commonly exhibit high selectivity but reduced permeability relative to the original, uncross-linked material [42,43].

Carbon molecular sieve (CMS) membranes derive from the pyrolysis of aromatic polymeric precursors. Because of the carbonization, CMS membranes possess a bimodal pore size distribution consisting of micropores (0.7–2 nm), which provide a high gas permeability, and ultramicropores (<0.7 nm), which allow a selective discrimination of gases by size molecular. This particular porous structure, which primarily depends on temperature, time of pyrolysis, treatment gas atmosphere, and precursor polymer, makes them ideal materials to separate gas pairs such as CO_2/CH_4, CO_2/N_2 and C_3H_6/C_3H_8 [44–46]. Several studies have shown the preparation of CMS membranes derived from blends of thermally stable and thermally labile polymers as an alternative to obtain higher permeability membranes, with better mechanical resistance, by controlled pyrolysis [47,48].

In a recent study [49], our group developed a strategy that consisted in blending a high-free volume aromatic polyimide with block aromatic-aliphatic copolymers, which derived from the same aromatic polyimide but with poly(ethylene oxide) (PEO) moieties incorporated to the main chain. 6FDA-6FpDA polyimide was chosen as the aromatic polymer because of its high free volume, good mechanical resistance and good permeability/selectivity balance for CO_2/CH_4 gas pair; however, this material suffers from plasticization. Blends of 6FDA-6FpDA polyimide and 6FDA-6FpDA-PEO copolyimide yielded cross-linked materials after selectively removing the PEO units upon thermal treatment below the degradation temperature of the aromatic polyimide. The cross-linked membranes exhibited better plasticization resistance to CO_2 relative to neat 6FDA-6FpDA polyimide. However, cross-linking caused a significant decrease in gas permeability, which was likely due to a volume shrinkage of membrane (i.e., a decrease in the fractional free volume (FFV)).

In this work, we propose a new strategy to eliminate the membrane volume shrinkage, consisting in the incorporation of an additional aromatic diamine, 3,5-diaminobenzoic acid (DABA), capable of producing interchain cross-linking [40,50,51]. Thus, during the thermal treatment to selectively remove the PEO units, an additional cross-linking due to the carboxylic groups takes place, which prevents, or minimizes the membrane shrinkage, leading to a much-improved permeability/selectivity balance.

To support this hypothesis, a series of aromatic copolyimides, 6FDA-6FpDA-DABA (PIx), and aromatic-aliphatic copolyimides, 6FDA-6FpDA-DABA-PEO (PIxEOy), has been prepared by varying the content of PEO and DABA. In this work, the content of PEO in the PIx/PIxEOy blends has been reduced to less than 10 wt%. These blends have been evaluated as gas separation membrane before and after a thermal treatment to remove the PEO units.

The final goal of this work is to use analogue cross-linkable materials as a mere additive that can be mixed with high free volume glassy polymers, to improve or maintain their gas separation properties, while enhancing their plasticization resistance.

2. Experimental

2.1. Materials

2,2′-Bis(4-aminophenyl)hexafluoropropane (6FpDA) was purchased from Chriskev (USA), and 4,4′-(hexafluoroisopropylidene) diphtalic anhydride (6FDA) and 3,5-diaminobenzoic acid (DABA) were purchased from Apollo Scientific (UK). These monomers were purified by high vacuum sublimation before use. Bis(2-aminopropyl) poly(ethylene oxide) (Jeffamine ED 2003), named here for simplicity as PEO, with a mean molecular weight of 1942 g/mol, was a gift from Huntsman International Europe. The PEO was dried to 40 °C for 5 h in a vacuum oven before use.

Anhydrous 1-methyl-2-pyrrolidone (NMP), anhydrous N, N′-dimethylacetamide (DMAc), anhydrous pyridine (Py), 4-dimethylaminopyridine (DMAP) and trimethylchlorosilane (TMSCl), and the other chemicals, such as acetic anhydride, were purchased from Sigma-Aldrich (Merck, Spain) with purity values above 99%.

2.2. Synthesis of aromatic copolyimides

Two aromatic copolyimides containing carboxyl groups were prepared by a two-step polycondensation reaction of equimolecular amounts of the 6FDA dianhydride and a mixture of the 6FpDA and DABA diamines in a mole ratio of 1/0.1 or 1/0.2. The reaction was carried out using a base-assisted *in-situ* silylation method, which has been shown as an efficient activation method to obtain high-molecular weight polyimides [52,53]. The reaction yield for all of the copolyimides was quantitative.

As an example, the synthesis of the PI10 copolyimide is described below:

A 100 mL three-neck flask equipped with a mechanical stirrer and gas inlet and outlet was charged with 7.50 mmol (2.50 g) of 6FpDA, 0.75 mmol (0.114 g) of DABA and 8 mL of NMP. Under blanket of nitrogen, the mixture was stirred at room temperature until the solid was completely dissolved, was cooled to 0 °C, and 18.1 mmol of TMSCl (2.30 mL) and 18.1 mmol (1.46 mL) of Py were added dropwise for 30 min. The solution was then stirred for 5 min and allowed to warm to room temperature to ensure the diamine silylation. Then, the solution was cooled again to 0 °C and 8.25 mmol (3.65 g) of 6FDA and 1.80 mmol (0.221 g) of DMAP were added together with 8 mL more of NMP. Following this step, the mixture was stirred for 15 min, the temperature was raised up to room temperature and the reaction was left overnight to form the poly(amic acid) solution. Afterward, 65.8 mmol (6.2 mL) of acetic anhydride and 65.8 mmol (5.3 mL) of Py were added and the mixture was stirred at room temperature for 6 h and at 60 °C for 1 h to promote the whole cyclization of poly(amic acid) to polyimide. Finally, the copolyimide was precipitated in distilled water, collected and consecutively washed with cold water, hot water and a water/ethanol

mixture (1/1) and finally dried in a vacuum oven at 60 °C for 12 h, at 120 °C for 1 h, and at 180 °C for 12 h.

For comparative purpose, the 6FDA-6FpDA and 6FDA-6FpDA-DABA polyimides were prepared from an equimolecular amount of 6FDA dianhydride and the corresponding diamine or diamines following the same methodology.

The 6FDA-6FpDA and 6FDA-6FpDA-DABA and the two copolyimides will be hereinafter referred to as PIx, where x is the percentage of DABA in the mixture of diamines. Thus, they will be named PI0, PI10, PI20 and PI100.

2.3. Synthesis of aromatic-aliphatic copolyimides

A series of aromatic-aliphatic copolyimides were prepared by a conventional two-step polycondensation reaction of equimolecular amounts of the 6FDA dianhydride and a mixture of the 6FpDA, DABA and PEO diamines. For the preparation of these copolyimides, mixtures with weight ratios (y/1) between the aromatic diamines (6FpDA and DABA) and the aliphatic diamine (PEO) of 1/1, 2/1 and 4/1 were used. In addition, the same mole ratios of 6FpDA and DABA in the mixture were used as in the aromatic copolyimides (1/0.1 and 1/0.2). Quantitative yields, well above 97%, were obtained for all of the copolymers.

As an example, the synthesis of the copolyimide using a 6FpDA/DABA molar ratio of 1/0.1 and a (6FpDA/DABA)/PEO weight ratio of 1/1 is described below:

A 100 mL three-neck flask equipped with a mechanical stirrer and nitrogen inlet and outlet was charged with 2.09 g (1.08 mmol) of dry PEO and 10 mL of NMP. When the PEO diamine was completely dissolved, 2.0 g (6.00 mmol) of 6FpDA and 0.091 g (0.60 mmol) of DABA were added together with 2 mL more of NMP. Once the diamines were dissolved, the flask was immersed in an ice-water bath and 7.68 mmol (3.40 g) of 6FDA dianhydride (in amount equimolar to the sum of the three diamines) and 10 mL more of NMP were added. The mixture was left stirring at room temperature for 12 h to form the poly(amic acid). Afterward, 60 mmol (5.65 mL) of acetic anhydride and 60 mmol (4.83 mL) of Py were added and the mixture was stirred at room temperature for 6 h and 60 °C for 1 h to promote the whole cyclization of poly(amic acid). Finally, the resulting copolyimide was precipitated into water and thoroughly washed in water and in ethanol-water 1/2 mixtures for several times, dried at 60 °C for 12 h, 120 °C for 1h, and 180 °C for 12 h under vacuum.

The aromatic-aliphatic copolyimides will be hereinafter referred as PIxEOy, where x is the molar percentage of DABA (x = 10 and 20) and y is weight ratio of aromatic diamine/aliphatic diamine mixture (y = 1, 2 and 4). As an example, the above copolyimide will be named as PI10EO1.

2.4. Membrane fabrication

2.4.1. Copolyimide membranes

Membranes of copolyimides were prepared via the solution casting method. 10% (w/v) copolyimide solutions in tetrahydrofuran (THF) were filtered through a 3.1 μm fiberglass Symta® syringe filter, poured onto a glass ring placed on a leveled glass plate, and left at 30 °C for 12 h and 60 °C for 12 h to remove most of the solvent. The films were peeled off from the glass plate and subjected to the following thermal treatment under vacuum conditions: 60 °C/1 h, 80 °C/30 min, 120 °C/1 h, 150 °C/30 min and 180 °C/12 h. Transparent films with thickness ranging from 40 to 60 μm were obtained.

2.4.2. Blend membranes

A series of blends were prepared using different weight ratios of PIx/PIxEOy copolyimides (z/1): 2/1 and 1/1. The required amounts of PIx and PIxEOy for each blend were dissolved at 10% (w/v) in THF by stirring at room temperature. Next, the films of the blends were obtained upon thermal treatment at 60 °C/1 h, 80 °C/30 min, 120 °C/1 h, 150 °C/30 min and 180 °C/12 h of flat membranes fabricated via the solution casting method.

The blends will be hereinafter referred as PIx/PIxEOy (z/1), where (z/1) is the weight ratio of PIx to PIxEOy.

2.4.3. Thermal cross-linking protocol

Samples of the copolyimides and blends were cut into 3 cm^2 pieces, sandwiched between two ceramic plates to avoid film curling at high temperatures and placed in a quartz tube furnace in a high-purity nitrogen atmosphere (0.3 L min^{-1}). Samples were heated to 275 °C at 10 °C min^{-1} and hold for 10 min, then to 375 °C at 5 °C min^{-1} and hold for 10 min, and finally to 400 °C at 5 °C min^{-1} for 1 min. Then, the samples were cooled as fast as device allowed (average cooling rate around 15 °C min^{-1}).

For the sake of simplicity, the cross-linked membranes will be named the same as the pristine membranes, but ending with TT. Thus, the key of abbreviations will be PIxEOy-TT and PIx/PIxEOy (z/1)-TT.

2.5. Characterization

^{1}H NMR spectra were recorded on Bruker Avance 400 spectrometer operating at 400 MHz in THF-d8. Attenuated total reflectance-Fourier transform infrared (ATR-FTIR) spectra were registered on a PerkinElmer Spectrum RX1 FTIR spectrometer. Inherent viscosities were measured at 30 °C with an Ubbelohde viscometer using DMAc as solvent at 0.5 g dL^{-1} concentration. Thermogravimetric analyses (TGA) were performed on a TA Q-500 thermobalance under a nitrogen atmosphere (60 mL min^{-1}). High-resolution dynamic thermogravimetric analyses (Hi-Res™ TGA) at 20 °C min^{-1} from 30 to 850 °C, with sensitivity and resolution parameters of 1 and 4, respectively, and isothermal TGA measurements by holding the sample at a given temperature for a given time were carried out. Wide-angle X-ray scattering (WAXS) patterns were recorded in the reflection mode at room temperature, using a Bruker D8 Advance diffractometer provided with a Goebel Mirror and a PSD Vantec detector. CuK_α (wavelength, $\lambda = 1.54$ Å) radiation was used. A step-scanning mode was employed for the detector, with a 2θ step of 0.024° and 0.5 s per step. The gel fraction of cross-linked samples was estimated using eq. (1):

$$\text{Gel fraction } (\%) = \frac{W_{\text{final}}}{W_{\text{initial}}} \text{ x } 100 \quad (1)$$

where W_{inital} is the weight of cross-linked sample and W_{final} is the weight of the cross-linked sample after extracting the soluble fraction. W_{final} was determined by immersing the cross-linked samples in DMAc at room temperature for 24 h and at 60 °C for 4 h under stirring. Then the sample was washed four times with ethyl ether and dried at 60 °C for 4 h and at 180 °C under vacuum for 12 h and weighed again. Mechanical properties were evaluated under uniaxial tensile tests at room temperature using an MTS Synergie-200 testing machine equipped with a 100 N load cell. Rectangular pieces of 5 mm width and 30 mm length were subjected to a tensile load applied at 5 mm min^{-1} until fracture.

2.6. Gas permeability measurement

Pure gas He, O_2, N_2, CH_4 and CO_2 permeability was measured at 35 °C and an upstream pressure of 3 bar using a constant volume/variable pressure apparatus. After the membrane was mounted in the permeation cell, both upstream and downstream chambers were exposed to full vacuum overnight to degas the membrane. The upstream pressure was adjusted to the desired value before starting the permeation experiment and, then, the pressure increase in the permeate side was recorded as a function of time. The permeability coefficient, P, was determined from the slope of downstream pressure vs time at steady-state:

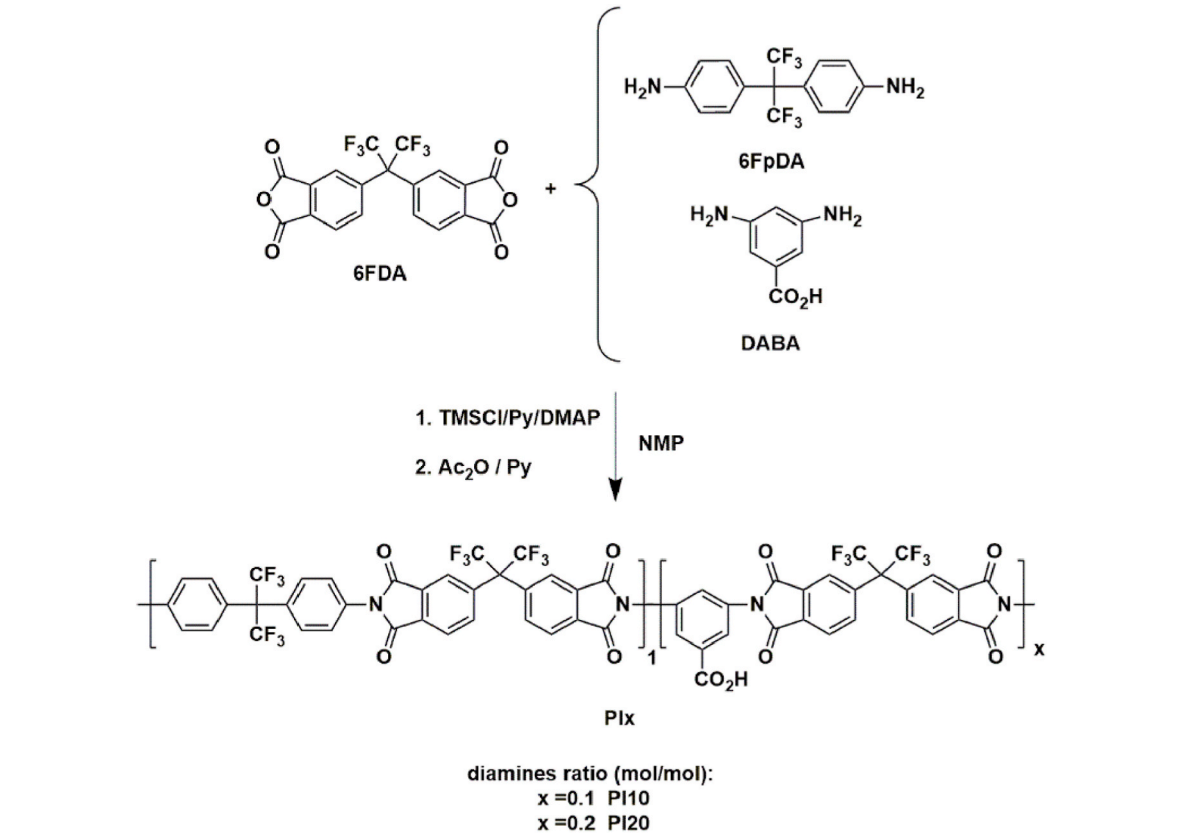

Fig. 1. Scheme of synthesis of the aromatic copolyimides (PIx).

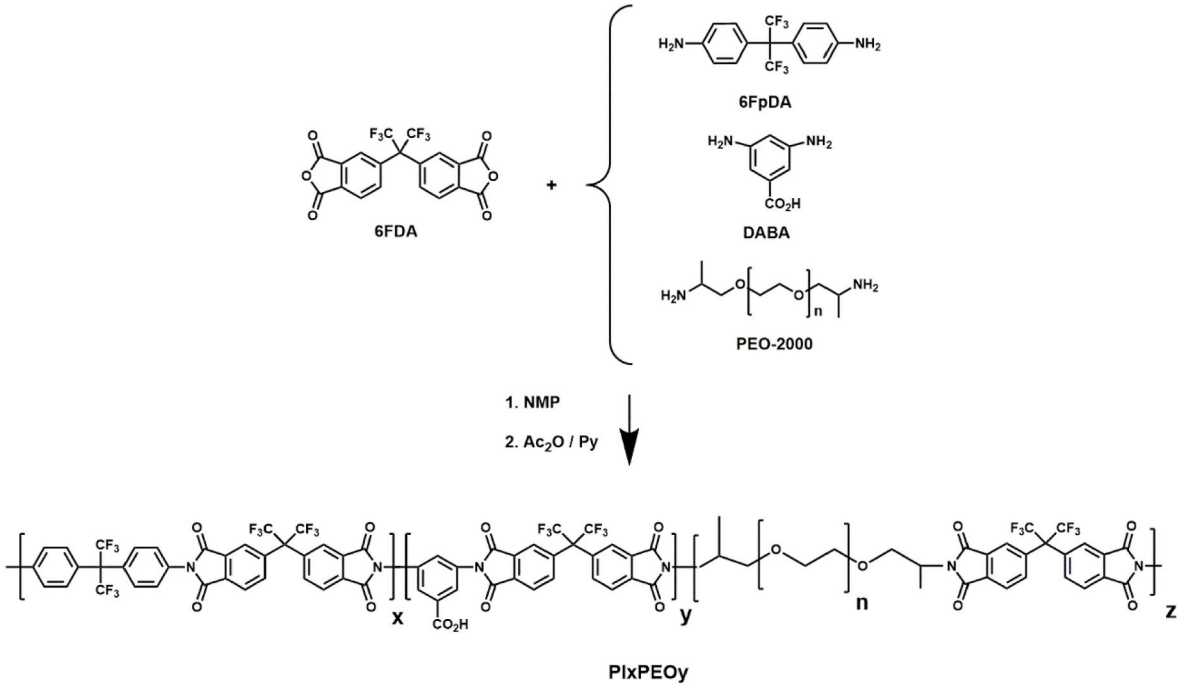

Fig. 2. Scheme of synthesis of aromatic-aliphatic copolyimides (PIxEOy).

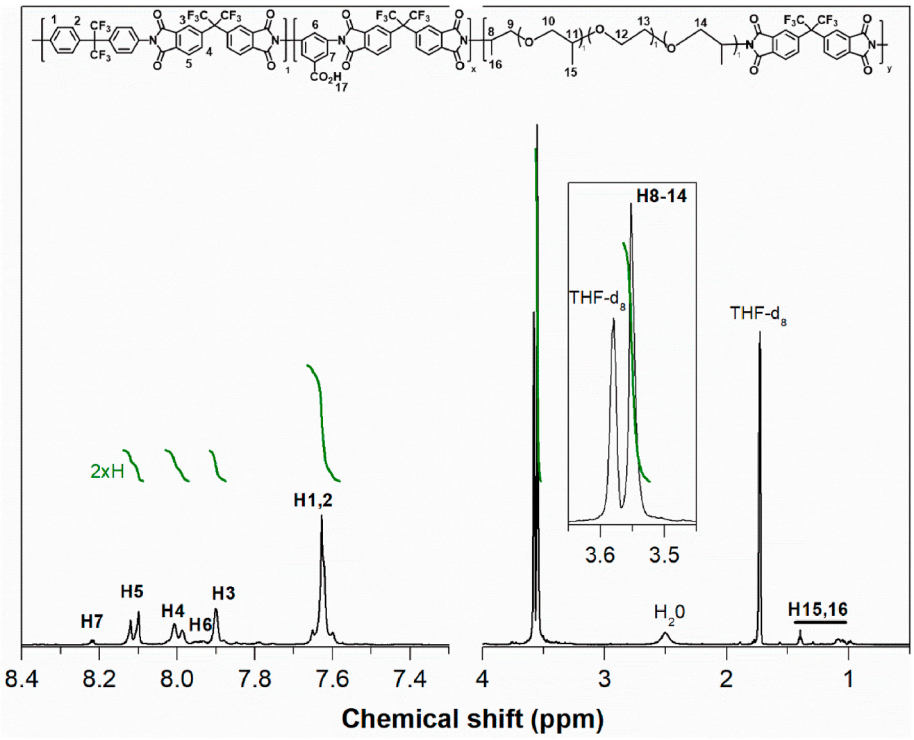

Fig. 3. ^{1}H NMR spectrum of PI20EO2 in THF-d_8.

Table 1
Inherent viscosity (η_{inh}) and thermogravimetric results of PI0 polyimide and PIx and PIxEOy copolyimides.

Sample	η_{inh}[a]	T_{d1}[b]	PEO content[d]	T_{d2}[b,c]	R_{800}[e]
PI0	0.703 ± 0.005		0	514	52.7
PI10	0.63 ± 0.01		0	512	53.0
PI10EO4	0.415 ± 0.004	394	9.93 (9.66)	nd[b]	46.9
PI10EO2	0.54 ± 0.01	383	19.0 (17.3)	nd[b]	42.2
PI10EO1	0.367 ± 0.006	376	30.8 (28.6)	nd[b]	36.0
PI20	0.363 ± 0.006		0	508	51.0
PI20EO4	0.472 ± 0.006	397	11.2 (9.45)	nd[b]	46.3
PI20EO2	0.508 ± 0.008	386	18.9 (17.0)	nd[b]	41.6
PI20EO1	0.40 ± 0.01	381	28.7 (28.1)	nd[b]	36.8

[a] measured in DMAc at 30 °C (dL g^{-1}), [b] the onset degradation temperatures (°C) of first (1) and second (2) weight loss steps, [c] the onset degradation temperature cannot be accurately determined by the overlap between the two steps (nd: not detected), [d] the parenthetical values correspond to the theoretical PEO content (wt%), and [e] the char yield at 800 °C (wt%).

$$P = \frac{273}{76}\frac{Vl}{ATp_0}\left[\left(\frac{dp(t)}{dt}\right)_{ss} - \left(\frac{dp(t)}{dt}\right)_{leak}\right] \quad (2)$$

where A and l are the effective area (cm^2) and the thickness of the membrane (cm), respectively, V is the volume of downstream chamber (cm^3), T is the temperature (K), p_0 is the pressure of the feed gas in the upstream chamber (bar), $(dp(t)/dt)_{ss}$ is the steady state rate of the pressure-rise (mbar s^{-1}), and $(dp(t)/dt)_{leak}$ is the system leak rate (mbar s^{-1}), which was less than 1% of $(dp(t)/dt)_{ss}$. P is expressed in Barrer [1Barrer = 10^{-10} (cm^3(STP) cm cm^{-2} s^{-1} $cmHg^{-1}$)]. The standard deviation was calculated considering three repeated experiments.

The selectivity (α) for a gas pair was calculated from the ratio of permeability coefficients of two gases (P_A and P_B) according to eq. (3).

$$\alpha = \frac{P_A}{P_B} \quad (3)$$

2.7. Plasticization test

The permeability to CO_2 and N_2 was sequentially measured at pressures of 1, 3, 5, 10, 15, 20, 25 and 30 bar and 35 °C. Each pressure step was run for 6 times the time lag followed by a depressurization step for approximately the same time. Then, the membrane was held at the highest pressure (30 bar) for 6 times the time lag followed by a depressurization step for 30 times the time lag. Finally, the measurement at 30 bar was repeated to check whether the permeability increased and the pressure was lowered stepwise and measured again to identify the hysteresis loop of the membrane. N_2 gas was measured first to exclude any plasticization or swelling effects.

3. Results and discussion

3.1. Synthesis and characterization of the copolyimides

A set of aromatic copolyimides (PIx) and aromatic-aliphatic copolyimides (PIxEOy) were prepared by a two-step condensation reaction as described in Experimental section. The chemical structure of the starting monomers and the synthetic scheme of the copolyimides are shown in Figs. 1 and 2. The activation of diamines by the in-situ silylation method was not used in the synthesis of PIxEOy, as this method yielded copolyimides with lower molecular weights than those obtained by the classical two-step polycondensation, i.e., performing the reaction between the diamine mixture and the dianhydride in a polar aprotic solvent. The compositions of all the copolyimides and the corresponding acronyms, which will be used throughout this paper, are shown in Table S1 in the Supporting Information (SI).

All of the copolyimides were soluble in polar aprotic media and even in a solvent like THF, as shown in Table S2 in the SI section, which allowed them to be easily processed into films using the casting method. Moreover, the use of THF as casting solvent greatly simplified the removal of solvent at low temperature.

The chemical structure of PIx and PIxEOy was confirmed by ^{1}H NMR and ATR-FTIR. As an example, the ^{1}H-NMR spectrum of PI20EO2 is

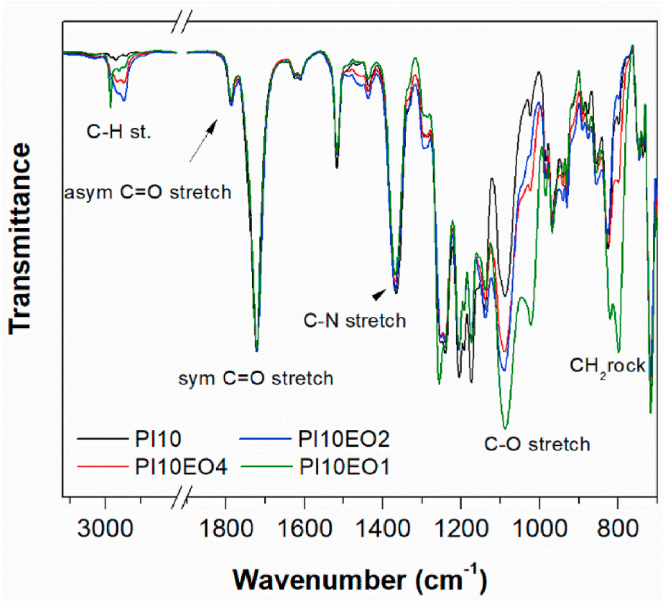

Fig. 4. ATR-FTIR spectra of PI10EOy copolyimides. The spectra were normalized to the band at 1720 cm^{-1} (sym C═O stretch).

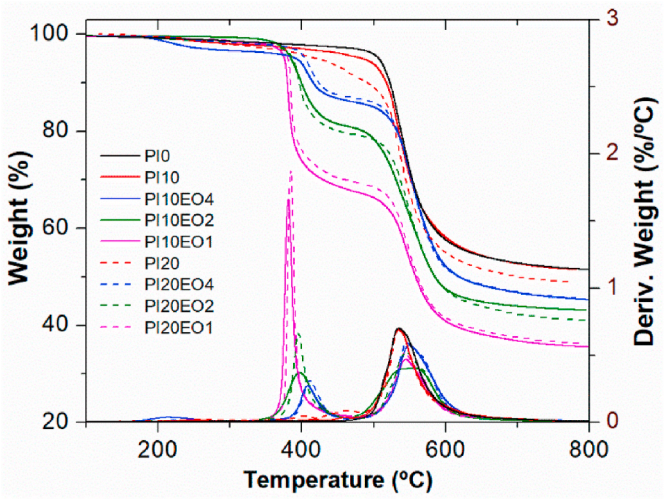

Fig. 5. Hi-Res TGA scans of PI0, PIx and PIxEOy under nitrogen atmosphere.

shown in Fig. 3. The characteristic peaks for aromatic protons appeared between 7.50 and 8.50 ppm. The protons of DABA moiety appeared at 8.22 (H7) and 7.95 ppm (H6). All the aromatic signals were consistent with the ones observed in the PI20 spectrum (Fig. S1 in SI section). The protons of methylene groups appeared at 3.52 ppm (H9, H10 and H12–H14) and the one of methyl groups between 1 and 1.5 ppm (H15 and H16). The composition of the copolyimides could not be accurately determined from the ratio of areas of the peaks at 8.22 and 7.95 ppm (of the DABA moiety) to the peak at 3.52 ppm (of the PEO fraction) because the integrated area under the aromatic peaks was considered too small to give a reliable value.

The molecular weight of copolyimides was estimated by measuring their inherent viscosities, and the values are listed in the first column of Table 1. It must be pointed out that the viscosities of PIx were not compared to those of PIxEOy because they have different chemical structures. For PIx, the viscosity and molecular weight decreased with increasing the DABA content. A possible explanation is the low reactivity of the amino groups from DABA monomer due to the electron-withdrawing effect of the carboxyl group, in spite of using the *in-situ*

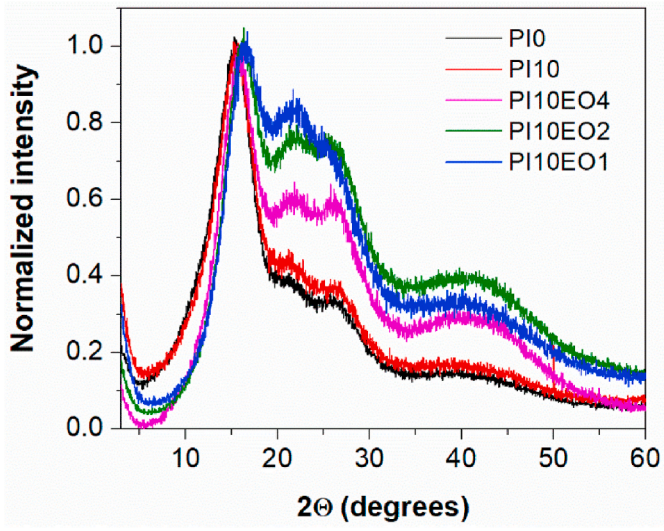

Fig. 6. WAXS patterns of PI0, PI10 and PI10EOy. For comparative purpose, the patterns were normalized to the intensity of the large scattering peak around 15.5° (2Θ).

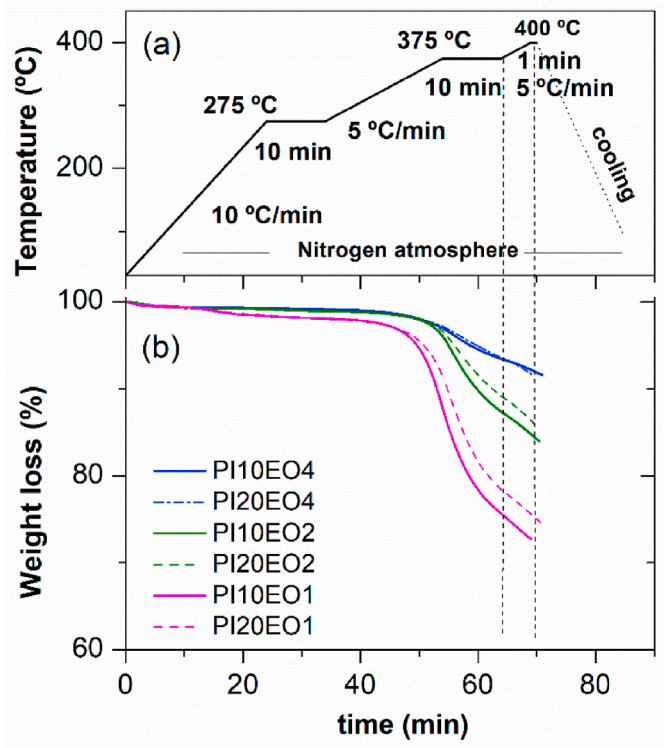

Fig. 7. (a) Scheme of the thermal treatment of cross-linking and (b) isothermal TGA curves for PIxEOy.

silylation method during the polyamic acid formation. For PIxEOy having comparable PEO percentages, the viscosities were similar, and thus similar molecular weights could have been achieved.

All of the copolyimides and the reference polyimide were processed as films, whose properties were thoroughly characterized to optimize the cross-linking protocol.

3.2. *Characterization of the membranes*

ATR-FTIR spectra of PIx and PIxEOy membranes are shown in Fig. 4 and Fig. S2 in the SI section. The characteristic absorption bands of

Table 2
Weight loss of PEO and gel fraction of PIxEOy-TT.

Sample	Exp. loss[a]	Exp. loss/Theor. Loss[b]	Gel fraction
PI10EO4-TT	7.73	80	90
PI10EO2-TT	14.7	85	92
PI10EO1-TT	25.4	89	68
PI20EO4-TT	7.92	84	85
PI20EO2-TT	13.5	80	82
PI20EO1-TT	23.4	83	77

[a] Experimental weight loss of PEO (%) after thermal treatment by TGA, [b] Experimental loss/theoretical loss ratio (%).

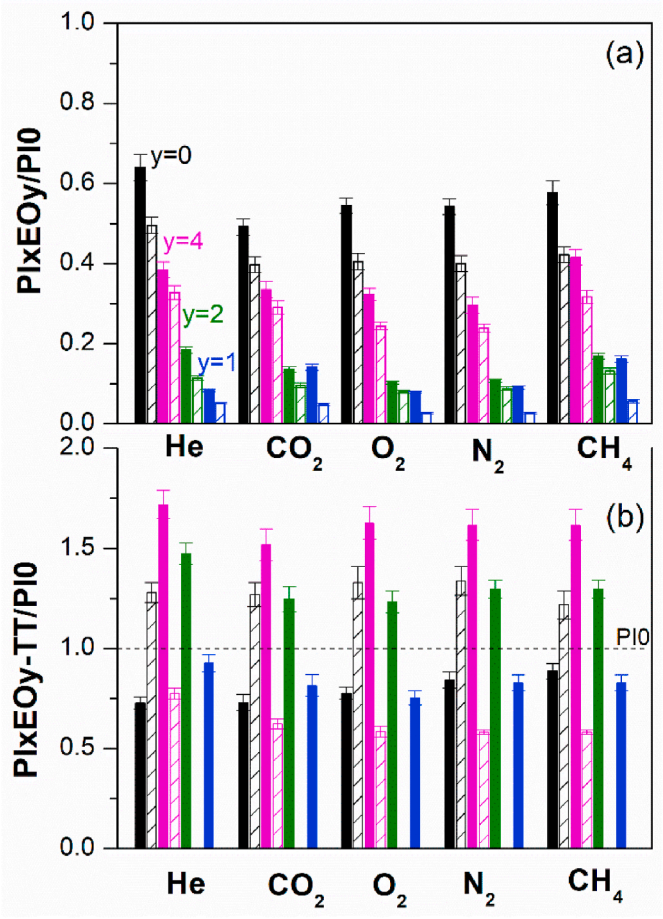

Fig. 8. Changes in permeability for PIx and PIxEOy, before (a) and after thermal treatment at 400 °C (b) relative to the neat PI0 (6FDA-6FpDA), which has been given a value of 1, for every tested gas at 35 °C. Solid column corresponds to x = 10 and cross-hatched column to x = 20. The standard deviations from repeated measurements are showed as error bars.

imide groups appeared at 1785 and 1720 cm^{-1} (C═O asymmetric and symmetric stretching, respectively) and 1360 cm^{-1} (C–N stretching). The typical aliphatic C–H absorption bands just below 3000 cm^{-1} were also detectable. Moreover, the intensity of the band centered at 1085 cm^{-1}, which was assigned to the C–O stretching mode of aliphatic ether moieties, and the bands around 810 cm^{-1}, which were related to the CH_2 rocking vibrations, increased with the higher PEO content.

The thermal stability of the copolyimide membranes was evaluated by TGA. The thermograms of PI0, PI10, PI20 and PIxEOy are shown in Fig. 5. In all of the copolyimides, a small weight loss below 300 °C (<3 wt%) was observed, which was attributed to residual solvent, indicating that the thermal treatment at 180 °C for 1 h was not enough to efficiently remove it. The degradation onset of PIx (i.e., around 450 °C) was found to be lower than that of PI0 (i.e., around 420 °C), which was attributed to the thermal decarboxylation of DABA prior to the polymer degradation. This thermal behavior has been already reported for other polymers containing DABA [50,51]. The thermograms of PI0 and PI100 (6FDA-DABA) were compared with those of PI10 and PI20 to support this fact, as shown in Fig. S3 in the SI section. It was observed that the loss weight by thermal decarboxylation in the PI100 (6FDA-DABA) covered the same temperature range, between around 350–500 °C, as in PIx. The decarboxylation mechanism over a wide temperature range would be consistent with removing of the carboxylic groups through a two-step mechanism including: the formation of interchain anhydride linkages and eventually cross-linking through decarboxylation (from dianhydride moieties and free carboxylic groups) at high temperature [51,54].

Two main weight losses were observed in the PIxEOy thermograms: a first one associated with the degradation of the PEO segments in the range between 350 and 450 °C -the higher the PEO content the higher the weight loss- and the other caused by the generalized degradation of the remaining polymer above 450 °C. In these copolyimides, the decarboxylation of the DABA moieties would occur during the last stage of degradation of the PEO segments.

The PEO content of PIxEOy was estimated by TGA from the weight loss of the first step. The percentage by weight of PEO, the onset degradation temperatures, T_{d1} and T_{d2}, which correspond to the PEO loss and the generalized degradation of polymer, respectively, and char yield at 800 °C of all the copolyimides are listed in Table 1. The calculated percentages of PEO group loss were somewhat higher than the theoretical ones because the existence of an overlap between the first and second stage of weight loss (due to the loss of DABA groups) did not allow a more accurate value to be obtained. As expected, the char yield of PIxEOy was lower than that of PIx because of the additional weight loss of PEO; thus, the higher the PEO content, the lower the char yield. Moreover, for the same content of DABA, Td_1 was found to be lower when the PEO content was higher.

WAXS was used to evaluate the effect of the PEO content on the membrane packing density. All of the patterns of PIx and PIxEOy exhibited amorphous halos indicating the amorphous nature of the membranes. The patterns of PI0, PIx and PIxEOy were compared in Fig. 6 and Fig. S4 in the SI section. The patterns of PIx were similar to that of PI0 exhibiting a high-intense well-defined scattering peak centered at 15.5° and three additional lower intensity peaks at 21.5, 26.5 and 40.0° (2Θ). According to Bragg's law (d-spacing = λ/sinΘ, where Θ is the scattering angle), the maxima' positions corresponded to preferential intersegmental distances (d-spacing) of 5.7, 4.1, 3.3 and 2.3 Å, respectively. This is in contrast to the patterns of PIxEOy that showed a slight shift of the highest intensity peak towards higher angles, for example from 15.5 for PI0 to 16.5° for PI10EO1, and a strong increase in the intensity of the other three peaks. This increase in intensity of the peaks was attributed to a higher contribution of the shorter d-spacing, especially those around 4.1 and 3.3 Å, to the global scattering pattern, indicating that PEO segments caused a higher packing density relative to that of PI0 and PIx.

3.3. Preparation of Cross-linked PIxEOy membranes

The thermal treatment to prepare the cross-linked membranes, PIxEOy-TT, was performed in a quartz tube furnace under a nitrogen atmosphere, and it was previously optimized by isothermal TGA measurements due to the wide temperature range where the removal of PEO took place (see Fig. 5). PIxEOy was crosslinked using a three-step thermal treatment, which is detailed in Fig. 7(a), along with the corresponding thermograms of the PIxEOy in Fig. 7(b). The residual solvent was removed in the first step, while the cross-linking of the samples took place in the other two ones. During the second step at 375 °C, the PEO weight loss, relative to the total PEO loss, for PIxEO1 was higher than 70%, while for PIxEO2 and PIxEO4 was lower because they seem to need

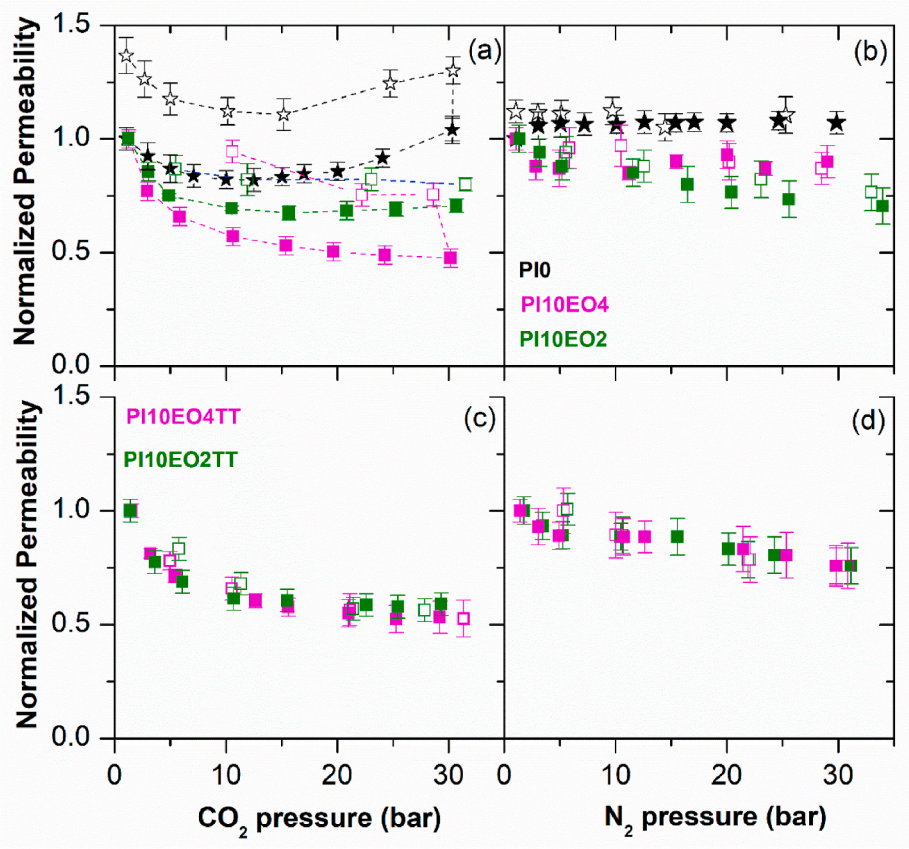

Fig. 9. Effect of CO_2 (a) and N_2 (b) pressure at 35 °C in reference polyimide (PI0) and precursor membranes (PI10EOy), and (c) and (d), respectively, in cross-linked membranes (PI10EOy-TT). The permeability was normalized to the initial value measured to a pressure of 1 bar. The standard deviations from repeated measurements are showed as error bars.

a higher temperature to remove the PEO, as shown in Fig. 5. Thus, the temperature was risen at 400 °C and the sample was held at that temperature for 1 min. With this last step, PEO weight losses of 80% or more were achieved for all the PIxEOy, as seen in Table 2. Moreover, according to the decarboxylation mechanism of DABA commented on above, it was expected that the additional cross-linking between adjacent acid groups would be due to the intermolecular anhydride formation, not by their loss, which would occur at higher temperatures (Fig. S3) [50,51,54,55].

The PEO removal was confirmed in addition to TGA by ATR-FTIR and X-ray diffraction, as an example seen in Figs. S5 and S6 in the SI section. It was observed that the aliphatic C–H absorption bands around 2950 cm^{-1} disappeared and the intensity of the C–O stretching band aliphatic ether moieties at 1085 cm^{-1} was significantly reduced. Thus, the spectra of the thermally treated were found to be similar to those of the corresponding PIx. The WAXS patterns of PIxEOy-TT were consistent with this result; similar WAXS patterns for PIxEOy-TT and PIx were observed.

The cross-linking of the PIxEOy after thermal treatment was checked by determining the gel fractions of PIxEOy-TT according to eq. (1). The values are listed in the last column of Table 2. It was found that the PIxEO1, having the highest PEO content, showed the lowest gel fractions (<80%), indicating a lower cross-linking degree than in the PIxEO4 and PIxEO2. Therefore, the higher the PEO content seems to hinder the cross-linking of the chains.

The mechanical properties of PIxEOy and PIxEOy-TT are listed in Table S3 in the SI section. Some examples of tensile stress vs strain plots are shown in Fig. S7. In general, the mechanical properties of PIxEO4 and PIxEO2 were similar to those of PI0, with Young's moduli about 2.0 GPa, tensile strengths higher than 85 MPa and moderate elongations at break from 7 to 12%. In particular, the mechanical properties of PI20EO1 were poorer than PI0, with a Young modulus of 1.0 GPa and tensile strength of 65 MPa. After thermal treatment, the mechanical properties of all the films decreased; especially for PIxEO1-TT and PI20EO2-TT, which could not be tested as gas separation membranes due to their poorer mechanical properties.

3.4. Gas transport properties

Pure gas He, O_2, N_2, CH_4 and CO_2 permeability in PIx, PIxEOy and their cross-linked analogs, PIx-TT and PIxEOy-TT, as well as the ideal selectivity for O_2/N_2 and CO_2/CH_4 gas pairs are listed in Table S4 of the SI section. For the sake of comparison, Fig. 8 shows the change in permeability of PIx and PIxEOy at 35 °C, before (a) and after (b) the thermal treatment at 400 °C, relative to the neat polyimide, PI0.

The gas permeability in PIx and PIxEOy before thermal treatment was significantly lower than that of PI0, to which the value of 1 was assigned, (cf. Fig. 8(a)). The decrease in permeability in PIx was associated with the formation of hydrogen bonds between carboxylic acids [55]; for example, the permeability was reduced by 50% in PI20. The reduction in permeability was considerably higher when the PEO content increased; this reduction was even higher in the membranes having the highest content of DABA, PI20EOy. The behavior of PIxEOy was consistent with the WAXS results where a higher packing was found for PIxEOy than for PI0, as shown in Fig. 6.

After the thermal treatment (cf. Fig. 8(b)), the permeability of the PIxEOy increased. However, only the permeability of PI10EO4-TT and PI10EO2-TT were higher than that of PI0. Although these cross-linked membranes showed similar WAXS patterns, the increase in He permeability of 1.72 times for PI10EO4-TT and 1.47 times for PI10EO2-TT

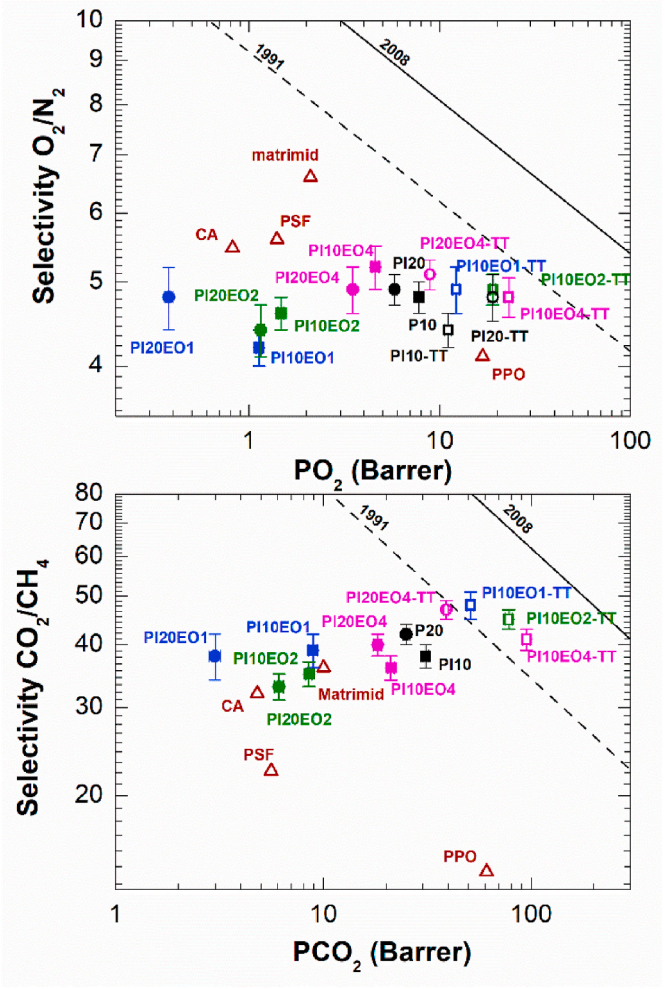

Fig. 10. O_2/N_2 (up) and CO_2/CH_4 (down) Robeson diagrams for PIxEOy and PIxEOy-TT. Continuous line represents the 2008 upper bound, and dashed line represents the 1991 upper bound. Data for relevant polymer used in gas separation were taken from Ref. [8] PSF: polysulfone (PSF); PPO: poly(phenyl oxide); CA: cellulose acetate, and Matrimid. The standard deviations from repeated measurements are showed as error bars.

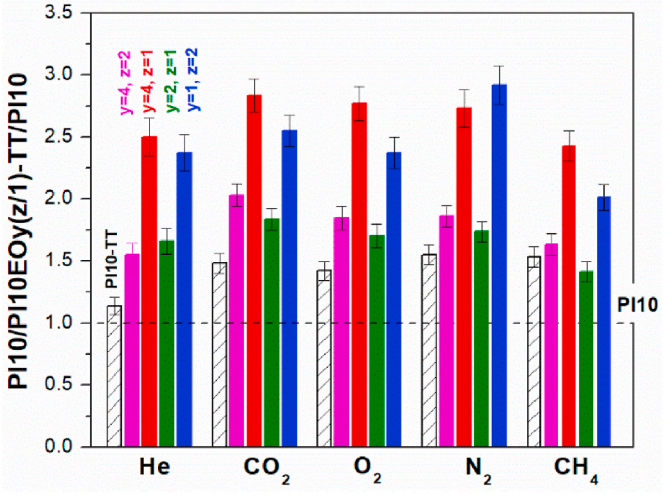

Fig. 11. Changes in permeability for PI10/PI10EOy(z/1) after thermal treatment at 400 °C relative to the neat polyimide, PI10, which was given a value of 1, as a function of tested gas at 35 °C. Solid column corresponds to x = 10 and cross-hatched column to PI10-TT. The standard deviations from repeated measurements are showed as error bars.

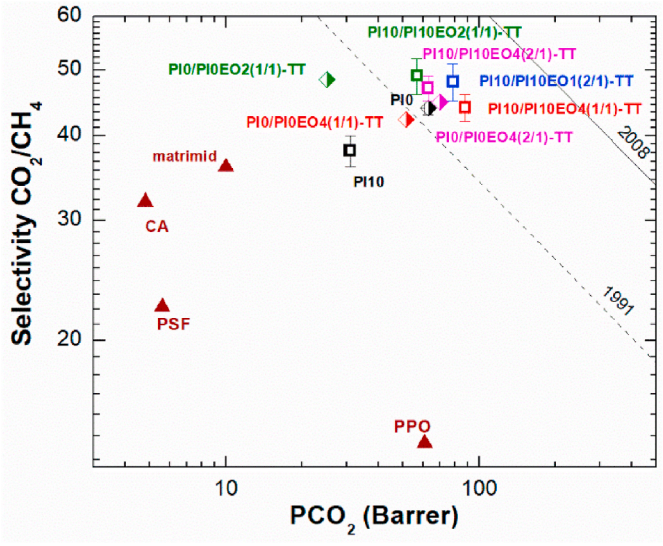

Fig. 12. CO_2/CH_4 Robeson diagram for PI10/PI10EOy-TT and PI0/PI0EOy-TT. Dashed line represents the 1991 upper bound and continuous line represents the 2008 upper bound. Data for relevant polymer used in gas separation were taken from Ref. [8]: polysulfone (PSF); poly(phenyl oxide) (PPO); cellulose acetate (CA), and Matrimid. The standard deviations from repeated measurements are showed as error bars.

relative to that of PI0 was associated with an increase in FFV due to the elimination of PEO during the thermal treatment. On the other side, the permeability of PI10EO4-TT was significantly higher than that of PI20EO4-TT, indicating that the presence of a higher DABA content in the membrane led to a lower FFV during the thermal treatment. This behavior was opposite to that observed in PIx, where the permeability of PI20 was higher than that of PI10 after thermal treatment.

Fig. 9 shows the normalized permeability behavior of CO_2 and N_2 as a function of feed pressure for PI10EO4 and PI10EO2 and their cross-linked analogs, as well as for PI0. The permeability to CO_2 of PI0 started to increase from a feed pressure about 12 bar due to the plasticization. Moreover, after holding the membrane to a feed pressure about 30 bar for a sufficient time (see Section 2.8), the permeability exhibited significant hysteresis when the feed pressure decreased. In contrast, N_2 did not induce plasticization or conditioning and, consistently with the dual mode picture [56], N_2 permeability slightly decreased as the feed pressure increased and no hysteresis was observed. PI10EO4 and PI10EO2 showed a similar behavior to that of PI0. After cross-linking, PI10EO4-TT and PI10EO2-TT exhibited resistance to CO_2-induced plasticization up to 30 bar.

To put these results in perspective, O_2/N_2 and CO_2/CH_4 separation performance of our membranes were compared with those of standard polymers used in membrane gas separation (cf. Fig. 10). The 1991 and 2008 upper bound lines are also included [15,16]. After the thermal treatment, the O_2/N_2 and CO_2/CH_4 separation performance of membranes shifted to the right, closer to the 1991 upper bound. PI10EOy-TT exhibited a higher O_2 permeability relative to PI10, without relevant O_2/N_2 selectivity loss. For example, O_2 permeability increased by 1.6-fold for PI10EO1-TT and by 2.9-fold for PI10EO4-TT. Interestingly, PI10EOy surpassed the 1991 CO_2/CH_4 upper bound. The CO_2/CH_4 separation performance for PI10EO4-TT and PI10EO2-TT was superior to that of PI10. Thus, for these two membranes, the permeability increased 2.5- and 3.0-fold and the selectivity between 1.1 and 1.2, respectively, compared to PI10.

3.5. Blends of PIx and PIxEOy

Considering that the PI10EOy-based cross-linked membranes showed the best separation performance for CO_2/CH_4, a series of membranes were prepared blending PI10 and PI10EOy at different weight ratios. The PI10/PI10EOy ratios were chosen such that the amount of PEO in the blends was between 3 and 10% (by weight). The blend films, PI10/PI10EOy(z/1), were obtained by solution casting and, then, they were subjected to the same thermal treatment described above (cf. Fig. 7). The removal of PEO in the blends was confirmed by TGA (cf. Fig. S8). The cross-linking degree was determined by measuring the gel fraction, which was higher than 90%. The composition of the blends and their acronyms, the percentage of PEO loss by weight after thermal treatment and the gel fraction are listed in Table S5 in the SI section.

The single gas permeability of the blends was measured at 30 °C and 3 bar before and after thermal treatment, and the data are shown in Tables S6 and SI section. Fig. 11 shows the variations in gas permeability of the cross-linked membranes relative to the pristine PI10. The relative gas permeability was higher in the cross-linked membranes derived from PI10-based blends than in the PI10-TT. It has to be pointed out that the thermal treatment on the PI10/PI10EO2(1/1), with a PEO content about 9.5 wt%, resulted in a less permeable membrane than those obtained from PI10/PI10EO1(2/1), which contained a higher percentage of PEO (about 10.5 wt%). This result seems to demonstrate that the mere PEO content in the blend is not the key point in determining the separation characteristics, but that the composition of PIxEOy, i.e., the content in PEO and DABA, is another crucial point to consider when designing new materials with this methodology.

The CO_2/CH_4 separation performance of PI10/PI10EOy(z/1)-TT is shown, in the Robeson plot, in Fig. 12. For the sake of comparison, the data for cross-linked membranes were compared to those of PI0-based analogous ones, which were reported in a previous work [49], and of their pristine PI10 and PI0. Because the composition of the precursor membranes (i.e., before the thermal treatment) were similar in both PI10-and PI0-series, analogous acronyms will be used to indicate them.

The cross-linking improved the CO_2/CH_4 separation performance of PI10/PI10EOy(z/1)-TT; both the permeability and selectivity of these membranes considerably increased relative to that of their reference polyimide, PI10. The performance of all the PI10/PI10EOy(z/1)-TT surpassed the 1991 upper bound. This behavior contrasted with that of PI0/PI0EOy(z/1) derived from the reference polyimide PI0; the PI0/PI0EOy(z/1)-TT showed similar, or even inferior, separation performance to that of PI0. For example, the CO_2 permeability of PI10/PI10EO4(1/1)-TT increased by 2.8-fold and its CO_2/CH_4 selectivity by 1.16-fold relative to PI10, while that of the analogue PI0/PI0EO4(1/1)-TT decreased by 0.8-fold and its selectivity barely varied relative to PI0. Therefore, the additional cross-linking from the carboxylic groups of DABA moieties in the PI10/PI10EOy(z/1) helps minimize the shrinkage exhibited by the PI0/PI0EOy(z/1) blends, while enhancing the selectivity/permeability balance relative to that of PI10.

4. Conclusions

A new strategy to obtain membranes with improved gas separation performance by selective removal of the PEO segments from the copolyimides, PIxEOy, containing carboxylic acids groups in their structure was successfully implemented and discussed. The incorporation of the DABA diamine in a molar percentage of 10% relative to 6FpDA diamine helped minimize the membrane shrinkage during the thermal removal of PEO. This effect was confirmed by a substantial improvement in O_2/N_2 and CO_2/CH_4 separations for thermally treated membranes. Moreover, the thermal cross-linking produced during the partial pyrolysis process greatly improved the plasticization resistance upon exposure to CO_2.

In this work, PI10/PI10EOy(z/1) blends have been prepared and their gas separation properties have been compared with those of their analogue PI0/PI0EOy(z/1) without DABA. The results showed that the presence of a small amount of DABA (molar percentage of 10% in both components of the blend) and PEO (less than 10 wt% relative to the total weight of the blend) significantly improved the separation performance relative to that of PI10 after the selective removal of PEO. The PI10/PI10EO4 (z/1) could have significant potential for CO_2/CH_4 separation application.

Speaking in a broader perspective, the methodology devised in this study to improve gas permeability while enhancing plasticization resistance is scalable and can be applied to other high FFV polymers, to enhance their separation performance and long-term stability.

Funding sources

This work was supported by the Spanish Government (AEI) through projects PID2019-109403RB-C21, PID2019-109403RB-C22 and PID2020-118547 GB-I00, and by the Regional Government of Castilla y León and the EU-FEDER program (CLU2017-09, UIC082, VA088G19 and VA224P20). M.G. acknowledges support of this work from the University of Oklahoma (VPR Office).

CRediT authorship contribution statement

Laura Matesanz-Niño: Validation, Investigation, Formal analysis, Writing – original draft. **Carla Aguilar-Lugo:** Validation, Investigation. **Pedro Prádanos:** Validation, Investigation, Funding acquisition. **Antonio Hernandez:** Validation, Investigation, Funding acquisition. **Camino Bartolomé:** Validation, Investigation, Formal analysis, Funding acquisition. **José G. de la Campa:** Methodology, Formal analysis, Resources. **Laura Palacio:** Validation, Formal analysis, Supervision, Funding acquisition. **Alfonso González-Ortega:** Validation, Methodology, Formal analysis, Supervision. **Michele Galizia:** Methodology, Resources, Writing – original draft, Writing – review & editing, Funding acquisition. **Cristina Álvarez:** Conceptualization, Methodology, Resources, Supervision, Writing – original draft, Writing – review & editing. **Ángel E. Lozano:** Conceptualization, Methodology, Resources, Writing – original draft, Writing – review & editing, Funding acquisition.

Declaration of competing interest

The authors declare that they have no known competing financial interests or personal relationships that could have appeared to influence the work reported in this paper.

Acknowledgments

L.M.N thanks the University of Valladolid for mobility grants UVa-2019 and UVa-2021, and the authors would like to thank Sara Rodriguez for her assistance with the gas separation measurements.

Appendix A. Supplementary data

Supplementary data to this article can be found online at https://doi.org/10.1016/j.polymer.2022.124789.

References

[1] D.S. Sholl, R.P. Lively, Seven chemical separations to change the world, Nature 532 (2016) 435–437, https://doi.org/10.1038/532435a.
[2] H. Lin, Integrated membrane material and process development for gas separation, Curr. Opin. Chem. Eng. 4 (2014) 54–61, https://doi.org/10.1016/j.coche.2014.01.010.
[3] M.E. Boot-Handford, J.C. Abanades, E.J. Anthony, M.J. Blunt, S. Brandani, N. Mac Dowell, J.R. Fernández, M.-C. Ferrari, R. Gross, J.P. Hallett, R.S. Haszeldine, P. Heptonstall, A. Lyngfelt, Z. Makuch, E. Mangano, R.T.J. Porter, M. Pourkashanian, G.T. Rochelle, N. Shah, J.G. Yao, P.S. Fennell, Carbon capture

and storage update, Energy Environ. Sci. 7 (2014) 130–189, https://doi.org/10.1039/C3EE42350F.
[4] M. Galizia, W.S. Chi, Z.P. Smith, T.C. Merkel, R.W. Baker, B.D. Freeman, 50th anniversary perspective : polymers and mixed matrix membranes for gas and vapor separation: a review and prospective opportunities, Macromolecules 50 (2017) 7809–7843, https://doi.org/10.1021/acs.macromol.7b01718.
[5] P. Bernardo, E. Drioli, G. Golemme, Membrane gas separation: a review/state of the art, Ind. Eng. Chem. Res. 48 (2009) 4638–4663, https://doi.org/10.1021/ie8019032.
[6] T.C. Merkel, H. Lin, X. Wei, R. Baker, Power plant post-combustion carbon dioxide capture: an opportunity for membranes, J. Membr. Sci. (2010), https://doi.org/10.1016/j.memsci.2009.10.041.
[7] P. Luis, T. Van Gerven, B. Van der Bruggen, Recent developments in membrane-based technologies for CO2 capture, Prog. Energy Combust. Sci. 38 (2012) 419–448, https://doi.org/10.1016/j.pecs.2012.01.004.
[8] D.F. Sanders, Z.P. Smith, R. Guo, L.M. Robeson, J.E. McGrath, D.R. Paul, B. D. Freeman, Energy-efficient polymeric gas separation membranes for a sustainable future: a review, Polymer 54 (2013) 4729–4761, https://doi.org/10.1016/j.polymer.2013.05.075.
[9] R.W. Baker, B.T. Low, Gas separation membrane materials: a perspective, Macromolecules 47 (2014) 6999–7013, https://doi.org/10.1021/ma501488s.
[10] Y. Ding, Perspective on gas separation membrane materials from process economics point of view, Ind. Eng. Chem. Res. 59 (2020) 556–568, https://doi.org/10.1021/acs.iecr.9b05975.
[11] Y. Yampolskii, Polymeric gas separation membranes, Macromolecules 45 (2012) 3298–3311, https://doi.org/10.1021/ma300213b.
[12] H.B. Park, J. Kamcev, L.M. Robeson, M. Elimelech, B.D. Freeman, Maximizing the right stuff: the trade-off between membrane permeability and selectivity, Science (2017) 356, https://doi.org/10.1126/science.aab0530.
[13] M. Rezakazemi, M. Sadrzadeh, T. Matsuura, Thermally stable polymers for advanced high-performance gas separation membranes, Prog. Energy Combust. Sci. 66 (2018) 1–41, https://doi.org/10.1016/j.pecs.2017.11.002.
[14] J. Deng, Z. Huang, B.J. Sundell, D.J. Harrigan, S.A. Sharber, K. Zhang, R. Guo, M. Galizia, State of the art and prospects of chemically and thermally aggressive membrane gas separations: insights from polymer science, Polymer 229 (2021), 123988, https://doi.org/10.1016/j.polymer.2021.123988.
[15] L.M. Robeson, Correlation of separation factor versus permeability for polymeric membranes, J. Membr. Sci. 62 (1991) 165–185, https://doi.org/10.1016/0376-7388(91)80060-J.
[16] L.M. Robeson, The upper bound revisited, J. Membr. Sci. 320 (2008) 390–400, https://doi.org/10.1016/j.memsci.2008.04.030.
[17] L.M. Robeson, Z.P. Smith, B.D. Freeman, D.R. Paul, Contributions of diffusion and solubility selectivity to the upper bound analysis for glassy gas separation membranes, J. Membr. Sci. 453 (2014) 71–83, https://doi.org/10.1016/j.memsci.2013.10.066.
[18] L.M. Robeson, Q. Liu, B.D. Freeman, D.R. Paul, Comparison of transport properties of rubbery and glassy polymers and the relevance to the upper bound relationship, J. Membr. Sci. 476 (2015) 421–431, https://doi.org/10.1016/j.memsci.2014.11.058.
[19] M. Minelli, G.C. Sarti, Elementary prediction of gas permeability in glassy polymers, J. Membr. Sci. 521 (2017) 73–83, https://doi.org/10.1016/j.memsci.2016.09.001.
[20] B.D. Freeman, Basis of permeability/selectivity tradeoff relations in polymeric gas separation membranes, Macromolecules 32 (1999) 375–380, https://doi.org/10.1021/ma9814548.
[21] C. Álvarez, A.E. Lozano, J.G. de la Campa, High-productivity gas separation membranes derived from pyromellitic dianhydride and nonlinear diamines, J. Membr. Sci. 501 (2016) 191–198, https://doi.org/10.1016/j.memsci.2015.11.039.
[22] P.M. Budd, N.B. McKeown, Highly permeable polymers for gas separation membranes, Polym. Chem. 1 (2010) 63, https://doi.org/10.1039/b9py00319c.
[23] I. Rose, C.G. Bezzu, M. Carta, B. Comesaña-Gándara, E. Lasseuguette, M.C. Ferrari, P. Bernardo, G. Clarizia, A. Fuoco, J.C. Jansen, K.E. Hart, T.P. Liyana-Arachchi, C. M. Colina, N.B. McKeown, Polymer ultrapermeability from the inefficient packing of 2D chains, Nat. Mater. 16 (2017) 932–937, https://doi.org/10.1038/nmat4939.
[24] Y. Okamoto, H.-C. Chiang, M. Fang, M. Galizia, T. Merkel, M. Yavari, H. Nguyen, H. Lin, Perfluorodioxolane polymers for gas separation membrane applications, Membranes 10 (2020) 394, https://doi.org/10.3390/membranes10120394.
[25] M. Yavari, M. Fang, H. Nguyen, T.C. Merkel, H. Lin, Y. Okamoto, Dioxolane-based perfluoropolymers with superior membrane gas separation properties, Macromolecules 51 (2018) 2489–2497, https://doi.org/10.1021/acs.macromol.8b00273.
[26] L.M. Robeson, M.E. Dose, B.D. Freeman, D.R. Paul, Analysis of the transport properties of thermally rearranged (TR) polymers and polymers of intrinsic microporosity (PIM) relative to upper bound performance, J. Membr. Sci. 525 (2017) 18–24, https://doi.org/10.1016/j.memsci.2016.11.085.
[27] I.M. Hodge, Physical aging in polymer glasses, Science 267 (1995) 1945–1947, https://doi.org/10.1126/science.267.5206.1945.
[28] R. Swaidan, B. Ghanem, E. Litwiller, I. Pinnau, Physical aging, plasticization and their effects on gas permeation in “rigid” polymers of intrinsic microporosity, Macromolecules 48 (2015) 6553–6561, https://doi.org/10.1021/acs.macromol.5b01581.
[29] Z.-X. Low, P.M. Budd, N.B. McKeown, D.A. Patterson, Gas permeation properties, physical aging, and its mitigation in high free volume glassy polymers, Chem. Rev. 118 (2018) 5871–5911, https://doi.org/10.1021/acs.chemrev.7b00629.
[30] F. Kadirkhan, P.S. Goh, A.F. Ismail, W.N.F. Wan Mustapa, M.H.M. Halim, W.K. Soh, S.Y. Yeo, Recent advances of polymeric membranes in tackling plasticization and aging for practical industrial CO2/CH4 applications—a review, Membranes 12 (2022) 71, https://doi.org/10.3390/membranes12010071.
[31] J.M. Hutchinson, Physical aging of polymers, Prog. Polym. Sci. 20 (1995) 703–760, https://doi.org/10.1016/0079-6700(94)00001-I.
[32] D. Cangialosi, V.M. Boucher, A. Alegría, J. Colmenero, Physical aging in polymers and polymer nanocomposites: recent results and open questions, Soft Matter 9 (2013) 8619, https://doi.org/10.1039/c3sm51077h.
[33] A. Bos, I.G.M. Pünt, M. Wessling, H. Strathmann, CO2-induced plasticization phenomena in glassy polymers, J. Membr. Sci. 155 (1999) 67–78, https://doi.org/10.1016/S0376-7388(98)00299-3.
[34] Y. Xiao, B.T. Low, S.S. Hosseini, T.S. Chung, D.R. Paul, The strategies of molecular architecture and modification of polyimide-based membranes for CO2 removal from natural gas-A review, Prog. Polym. Sci. 34 (2009) 561–580, https://doi.org/10.1016/j.progpolymsci.2008.12.004.
[35] A. Bos, I. Pünt, H. Strathmann, M. Wessling, Suppression of gas separation membrane plasticization by homogeneous polymer blending, AIChE J. 47 (2001) 1088–1093, https://doi.org/10.1002/aic.690470515.
[36] S. Mazinani, R. Ramezani, G.F. Molelekwa, S. Darvishmanesh, R. Di Felice, B. Van der Bruggen, Plasticization suppression and CO2 separation enhancement of Matrimid through homogeneous blending with a new high performance polymer, J. Membr. Sci. 574 (2019) 318–324, https://doi.org/10.1016/j.memsci.2018.12.060.
[37] W.F. Yong, F.Y. Li, T.S. Chung, Y.W. Tong, Molecular interaction, gas transport properties and plasticization behavior of cPIM-1/Torlon blend membranes, J. Membr. Sci. 462 (2014) 119–130, https://doi.org/10.1016/j.memsci.2014.03.046.
[38] K. Vanherck, G. Koeckelberghs, I.F.J. Vankelecom, Crosslinking polyimides for membrane applications: a review, Prog. Polym. Sci. 38 (2013) 874–896, https://doi.org/10.1016/j.progpolymsci.2012.11.001.
[39] S.D. Kelman, B.W. Rowe, C.W. Bielawski, S.J. Pas, A.J. Hill, D.R. Paul, B. D. Freeman, Crosslinking poly[1-(trimethylsilyl)-1-propyne] and its effect on physical stability, J. Membr. Sci. 320 (2008) 123–134, https://doi.org/10.1016/j.memsci.2008.03.064.
[40] H. Eguchi, D.J. Kim, W.J. Koros, Chemically cross-linkable polyimide membranes for improved transport plasticization resistance for natural gas separation, Polymer 58 (2015) 121–129, https://doi.org/10.1016/j.polymer.2014.12.064.
[41] W.F. Yong, K.H.A. Kwek, K.-S. Liao, T.-S. Chung, Suppression of aging and plasticization in highly permeable polymers, Polymer 77 (2015) 377–386, https://doi.org/10.1016/j.polymer.2015.09.075.
[42] M. Puertas-Bartolomé, M.E. Dose, P. Bosch, B.D. Freeman, J.E. McGrath, J.S. Riffle, A.E. Lozano, J.G. De La Campa, C. Álvarez, Aromatic poly(ether ether ketone)s capable of crosslinking via UV irradiation to improve gas separation performance, RSC Adv. 7 (2017), https://doi.org/10.1039/c7ra11018a.
[43] M. Askari, T.-S. Chung, Natural gas purification and olefin/paraffin separation using thermal cross-linkable co-polyimide/ZIF-8 mixed matrix membranes, J. Membr. Sci. 444 (2013) 173–183, https://doi.org/10.1016/j.memsci.2013.05.016.
[44] K.M. Steel, W.J. Koros, An investigation of the effects of pyrolysis parameters on gas separation properties of carbon materials, Carbon N. Y. 43 (2005) 1843–1856, https://doi.org/10.1016/j.carbon.2005.02.028.
[45] M. Kiyono, P.J. Williams, W.J. Koros, Effect of polymer precursors on carbon molecular sieve structure and separation performance properties, Carbon N. Y. 48 (2010) 4432–4441, https://doi.org/10.1016/j.carbon.2010.08.002.
[46] J.S. Adams, A.K. Itta, C. Zhang, G.B. Wenz, O. Sanyal, W.J. Koros, New insights into structural evolution in carbon molecular sieve membranes during pyrolysis, Carbon N. Y. 141 (2019) 238–246, https://doi.org/10.1016/j.carbon.2018.09.039.
[47] M.E. Rezac, E. Todd Sorensen, H.W. Beckham, Transport properties of crosslinkable polyimide blends, J. Membr. Sci. 136 (1997) 249–259, https://doi.org/10.1016/S0376-7388(97)00170-1.
[48] Y.-J. Fu, C.-C. Hu, D.-W. Lin, H.-A. Tsai, S.-H. Huang, W.-S. Hung, K.-R. Lee, J.-Y. Lai, Adjustable microstructure carbon molecular sieve membranes derived from thermally stable polyetherimide/polyimide blends for gas separation, Carbon N. Y. 113 (2017) 10–17, https://doi.org/10.1016/j.carbon.2016.11.026.
[49] L. Escorial, M. de la Viuda, S. Rodríguez, A. Tena, A. Marcos, L. Palacio, P. Prádanos, A.E. Lozano, A. Hernández, Partially pyrolized gas-separation membranes made from blends of copolyetherimides and polyimides, Eur. Polym. J. 103 (2018) 390–399, https://doi.org/10.1016/j.eurpolymj.2018.04.031.
[50] E.M. Maya, A. Tena, J. de Abajo, J.G. de la Campa, A.E. Lozano, Partially pyrolyzed membranes (PPMs) derived from copolyimides having carboxylic acid groups. Preparation and gas transport properties, J. Membr. Sci. 349 (2010) 385–392, https://doi.org/10.1016/j.memsci.2009.12.001.
[51] A.M. Kratochvil, W.J. Koros, Decarboxylation-induced cross-linking of a polyimide for enhanced CO 2 plasticization resistance, Macromolecules 41 (2008) 7920–7927, https://doi.org/10.1021/ma801586f.
[52] D.M. Muñoz, J.G. de la Campa, J. de Abajo, A.E. Lozano, Experimental and theoretical study of an improved activated polycondensation method for aromatic polyimides, Macromolecules 40 (2007) 8225–8232, https://doi.org/10.1021/ma070842j.
[53] D.M. Muñoz, M. Calle, J.G. de la Campa, J. de Abajo, A.E. Lozano, An improved method for preparing very high molecular weight polyimides, Macromolecules 42 (2009) 5892–5894, https://doi.org/10.1021/ma9005268.

[54] C. Zhang, P. Li, B. Cao, Decarboxylation crosslinking of polyimides with high CO2/CH4 separation performance and plasticization resistance, J. Membr. Sci. 528 (2017) 206–216, https://doi.org/10.1016/j.memsci.2017.01.008.
[55] C. Staudt-Bickel, W.J. Koros, Improvement of CO2/CH4 separation characteristics of polyimides by chemical crosslinking, J. Membr. Sci. 155 (1999) 145–154, https://doi.org/10.1016/S0376-7388(98)00306-8.
[56] M. Saberi, A.A. Dadkhah, S.A. Hashemifard, Modeling of simultaneous competitive mixed gas permeation and CO2 induced plasticization in glassy polymers, J. Membr. Sci. 499 (2016) 164–171, https://doi.org/10.1016/j.memsci.2015.09.044.